Thermal strain extraction methodologies for bridge structural condition assessment

Thermal strain extraction methodologies for bridge structural condition assessment

To cite this article before publication: Yanjie Zhu *et al* 2018 *Smart Mater. Struct.* in press https://doi.org/10.1088/1361-665X/aad5fb

Thermal Strain Extraction Methodologies for Bridge Structural Condition Assessment

Author 1:
Yanjie Zhu, PhD student
Civil Research Group, School of Engineering, University of Warwick, UK
Yanjie.Zhu@warwick.ac.uk

Author 2:
Yi-Qing Ni, Professor
Department of Civil and Environmental Engineering, The Hong Kong Polytechnic University, Hong Kong

Author 3:
Andre Jesus, Teaching Fellow
Civil Research Group, School of Engineering, University of Warwick, UK

Author 4:
Jingliang Liu, Assistant Professor
School of Transportation and Civil Engineering, Fujian Agriculture and Forestry University, China

Author 5:
Irwanda Laory, Associate Professor
Civil Research Group, School of Engineering, University of Warwick, UK
I.Laory@warwick.ac.uk

* Corresponding authors: Irwanda Laory (I.Laory@warwick.ac.uk)

Acknowledgements
The first author gratefully acknowledges financial support from University of Warwick and China Scholarship Council.

Thermal Strain Extraction Methodologies for Bridge Structural Condition Assessment

Abstract

This paper presents a feature extraction method to uncover the temperature effects on bridge responses, which combines mode decomposition, data reduction and blind separation. For mode decomposition, empirical mode decomposition (EMD) and ensemble empirical mode decomposition (EEMD) have been selected, followed by principal component analysis (PCA) for data size compression. The independent component analysis (ICA) is then employed for blind separation. The unique feature of the proposed method is the blind separation, which means temperature-induced response can be extracted from the mixed structural responses, without any prior information of the loading conditions and structural physical models. This study further evaluates the effects of extracting temperature-induced response on damage detectability when using Moving Principal Component Analysis (MPCA). The numerical analysis of a truss bridge is first used to evaluate the proposed method for thermal feature extraction, followed by a real truss bridge test in the structural laboratory in University of Warwick. Results from the numerical case study show that the method enables the separation of temperature-induced response, and furthermore, the EEMD, in mode decomposition, has a positive influence on the blind separation than EMD, when combined with PCA and ICA. Finally, the real truss bridge test demonstrates that the feature extraction method can enhance the probability of MPCA to uncover the damage, as the MPCA fails without proposed method.

Keywords: Blind separation; Damage detection; Mode decomposition; Structural health monitoring; Thermal effect

1 Introduction

The structural health monitoring system is designed to monitor critical civil structures, e.g. long-span bridges and skyscrapers, and to assess their in-service performance. Several main purposes of SHM are summarized as: to provide update on bridge condition during construction stage; to monitor structural operational performance under real loading conditions; to detect damage or deterioration and thereby give guidelines of maintenance activities. The structural condition assessment, using model-free techniques, can be fundamentally considered as statistical pattern recognition problems [1], which is capable to predict adverse effects by detecting damage-induced discrepancy among structural responses. The motivations and applications of SHM in twentieth century have been summarized by Sohn [2] and Brownjohn [3]. Recent development can be found in [1,4,5] especially those critical complex civil structures [6]. There are also some papers addressing structural health monitoring applications on bridge structures, such as [7–10].

To assess structural condition, i.e. damage detection and deterioration monitoring, the SHM technique should analyse the structural response of interest. However, bridge physical measurements are exposed to complicated surroundings in the service. Thermal loading, together with structural loading and others, can also change structural characteristics. Sohn [11] had offered a comprehensive summary of previous findings that temperature can affect structural properties, such as material properties [12], structural boundary conditions [13] and structural dynamic behaviours [14]. Moreover, it is highly possible that the wiggling in static response of interest can be covered by the structural changes due to temperature fluctuation. For example, Nguyen et al. pointed out stiffness of asphalt and bearings can be influenced by solar irradiation which then affects static test results [15]. Helmicki et al. reported that the temperature drives much more stresses than traffic [16]. Similarly, Catbas et al. observed that the maximum temperature-induced strain is around ten times higher than maximum traffic-induced strains, based on the one-year monitoring data of a long span truss bridge in the United States [17]. The impact of temperature and train loadings have been distinguished clearly by Cross et al. that temperature is a dominant contributor for seasonal fluctuations in the modal frequencies, while train loading is an important driver of daily variations [18]. The latest research on the large-span gymnasium in China also

demonstrated that the environmental variations, especially temperature, are obstacles for structural reliability assessment and highly efficient long-term health monitoring [6].

To identify the thermal impact, most previous researches followed the idea of formulating the function between structural parameters and measurable temperature distributions, along with eliminating temperature influence. The statistical regression analysis and artificial intelligence technique are the popular methods for establishing temperature influence model. For example, with measurable temperature data, Peeters and De Roeck established an eigenfrequency-temperature relation model [14]. This model is based on Auto-regressive and Exogenous (ARX) model from healthy bridge monitoring data. Then this ARX-based model can estimate confidence intervals for eigenfrequency. If a newly recorded eigenfrequency exceeds the estimated confidence intervals, which is simulated by ARX-based model, then the damage can be detected. However, the application on Z-24 Bridge in Switzerland did not consider temperature under freezing point, which makes ARX-based model unable to successfully detect damage below zero degree centigrade. After that, Ding and Li proposed a polynomial regression model to study the relationship between modal frequency and temperature, considering daily and seasonal temperature variation individually [19]. This model was then employed on Runyang Suspension Bridge in China for removing daily temperature effects on frequency. Similarly, Jin *et al.* combined statistical regression method with neural network algorithm on a US highway bridge [20]. The dependency of structural natural frequency upon temperature variable was studied by time series analysis method based on the one-year monitoring data. Dependent on the temperature-frequency relation, the proper variables are selected for training neural network afterwards. In recent years, Kromanis and Kripakaran utilized the measurable structural responses and temperature distributions to develop a regression-based thermal response prediction model, termed as RBTRP methodology [21]. The predicting model is subsequently coupled with anomaly detection methodologies to characterize the response changes by comparing measured and predicted bridge behaviour, named as Temperature-based Measurement Interpretation (TB-MI) [22]. Yarnold et al. have proposed a temperature-driven method, in which the 3D relation, or signature, among temperature variable, mechanical strains and structural displacements was identified [10,23]. In addition, Zhou et al. have also summarized previous efforts devoted to investigating temperature contributions since 1960s [24].

However, there are some cases in which temperature measurement is unavailable. In this situation, directly distinguishing temperature-induced changes from mixed structural response is a critical issue. Previous attempt was given by Sohn et al. [25]. They proposed to extract damage-sensitive feature from the structural system responses that contains wild range environmental conditions. The selected feature will be used as input for an auto-associative neural network, while the unmeasured environmental conditions were treated as hidden intrinsic parameters. The underlying association between the selected damage-sensitive feature and structural system, including environmental effects, can be characterized by the neural network. The drawbacks of this method are apparent and as follow. The training data set, where the damage-sensitive feature comes from, should contain as many environmental variations as possible, however, this is blurry and hard to achieve. Moreover, if the training data miss some unusual environmental conditions, the proposed method cannot make correct alarm when the structural system is in these unusual situations. The other attempts have conducted by Yan et al. [26] and Bellino et al. [27], who leveraged principal component analysis (PCA) for eliminating environmental effects on vibration features. Wah et al. also employed PCA on natural frequencies to cluster the observations based on their environmental conditions [28]. And further damage detection is within each cluster to avoid temperature influence.

This paper proposes to extract thermal strain from mixed structural response for the subsequent damage detection process. The separation is combining mode decomposition and blind source separation methods. The thermal strain is the structural response under temperature load effect only, while the mixed structural response represents the structural responses under various loading conditions. The idea of proposed feature extraction method comes from the basic theory that various loadings produce the corresponding response signals with specific characteristics, for example, thermal stresses produced by ambient temperature is more evident and changing slowly when compared with stresses caused by wind or heavy traffic loadings. The proposed feature extraction method will be described as a federation of the mode decomposition, the data reduction and the blind separation. For mode decomposition of target

signal, empirical mode decomposition (EMD) and ensemble empirical mode decomposition (ensemble EMD or EEMD) will be employed, followed by principal component analysis (PCA) to compress the data size before performing independent component analysis (ICA) for final separation. The extracted temperature response is then applied for damage detection, where moving principal component analysis (MPCA) will be applied.

Both EMD and EEMD have been utilized as an assistant tool to support the fault detection, for example, Miao et al. [29] employed EMD and Žvokelj et al. [30] utilized EEMD for bearing failure detection. Empirical mode decomposition (EMD) and ensemble empirical mode decomposition (EEMD) have been widely employed in vibration-based structural health monitoring, but not considering temperature effects. Such as, Yang et al. demonstrated that EMD is capable of detecting damage, reflected as sudden spikes in first intrinsic mode function separated by EMD [31]. However, the successful applications are based on the following assumptions: the structural acceleration is not polluted by noise and damage induces an abrupt change in stiffness value. Those hypotheses are really difficult to achieve in practice. OBrien et al. proposed to apply EMD to decompose vehicle driven responses for damage detection and location [32]. As previous research has demonstrated that a passing vehicle loading can activate three main components in mixed responses, which are vehicle frequency, bridge natural frequency and the vehicle-induced frequency [33]. Among those components, the vehicle-induced frequency is more sensitive to damage and has potential to locating the damage [34]. Other applications of EMD and EEMD for damage detection have been summarized in [35]. However, above applications did not consider temperature variations. The EMD and EEMD in this paper is utilized to assist the process of blind separation in order to extract thermal features.

PCA is a statistic data interpretation method for compressing the size of a dataset by transforming it to a principal component space. According to Jolliffe [36], PCA was first formulated by Peason in 1901 and Hotelling [37]. For some researches, PCA is mainly used to eliminated the impact of environmental variations [27,28]. PCA has also been widely used in sensor fault diagnosis [38,39]. But in this study, the main function of PCA is data dimension reduction, which can be found in some other papers [40,41].

The Independent Component Analysis (ICA) employed in this study is the most popular solution for Blind Source Separation (BSS) problem. A comprehensive summary of the applications of blind separation for mode identification have been summarized by Sadhu et al. [42]. More researches of blind separation skills on structural dynamics can be found in [43,44]. The original idea of ICA was first proposed by Comon [45], which is to maximize the statistical independence among its separated components by performing a linear transformation on the target data. There are some applications that leverage ICA along with other techniques for structural identification or damage detection. For instance, ICA was employed with artificial neural network for detecting damage diagnosis [46]. The authors decomposed time history records into a set of independent components and the mixing matrix. And treat the mixing matrix as the representation of structural vibration features. The two parts of ICA output are subsequently utilized to build a neural network model, as an indicator for detecting damage. Poncelet et al. applied ICA to estimate the damping ratios and modal frequencies in mechanical systems [47]. The applications mentioned above do not take temperature influence in consideration. In this study, the ICA will be leveraged for extracting mechanical strain induced by seasonal and daily temperature respectively. Yang and Nagarajaiah combined wavelet transform with ICA to obtain the recovered mixing matrix, which contains interesting damage information [48]. More application of ICA for mode identification based on dynamic characteristics can be found in [48,49]. ICA has also been employed into various fields, for example, in the field of process monitoring and control [50–52], in the bearing fault detection [30,53].

In the final damage detection process, moving principal component analysis, abbreviated as MPCA, is employed. MPCA was first proposed by Posenato et al. in 2008 as an improved statistical method of PCA [54]. If applying PCA on continuous monitoring data directly, two drawbacks exist which cannot be ignored. The first is the computation cost due to the covariance matrix calculation. As the number of measurements increases, the effect of new points in the covariance matrix is lower and lower because they are averaged by the total number of points, i.e. the first normalization procedure in PCA. To solve this problem, the recursive strategy can be adapted to reveal anomalous variations among long-term

monitoring [55]. Relevant researches that investigated MPCA for damage detection can be found in [56–58].

There are three unique key factors in this research.

- It is a non-parametric method for extracting features from an unknown structural system. In another word, there is no need for prior knowledge of the in-service conditions and structural physical models;
- In previous researches, EMD, EEMD, PCA and ICA have been applied individually or combined with others for various research purposes, which will be summarized in next section. However, it is the first time to combine these three approaches as a feature extraction method for extracting temperature-induced responses;
- It is a new idea to assess the capability of using temperature-induced responses for damage detection.

The rest of this paper is organized as follows. Section 2 will introduce proposed blind separation method, in the order of mode decomposition (i.e. EMD and EEMD) in Section 2.1, data reduction (i.e. PCA) in Section 2.2 and blind separation (ICA) in Section 2.3. Since there have two choices in mode decomposition stage, EMD and EEMD, the proposed solution scheme can be abbreviated as EPI and EEPI, which represent the combination of EMD+PCA+ICA and EEMD+PCA+ICA respectively. Afterwards, a brief description of the damage detection method, moving principal analysis (MPCA) will be given in Section 2.4. The numerical case study on a down scaled truss bridge model will be presented in Section 3, followed by a down scaled truss bridge lab study in Section 4. The conclusion is summarized at the end of the paper (Section 5).

2 Methodology

The general idea of the proposed method can be found in Fig. 1. The proposed thermal feature extraction method is first applied on structural responses and the extracted sources of interest are subsequently used for structural assessment. Specifically, the feature extraction method is a combination of mode decomposition, data reduction and blind separation, which will be described in the next three sub-sections, followed by the algorithm for damage detection in Section 2.4.

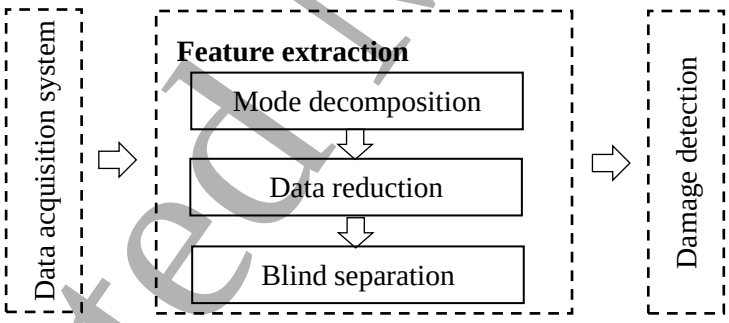

Fig. 1. Outline of the proposed method

2.1 Mode decomposition

The mode decomposition can be viewed as an expansion of the single-channel target data. The empirical mode decomposition (EMD), proposed by Huang et al in 1998 [59], is used to decompose a single-channel data, while the ensemble empirical mode decomposition (EEMD), developed by Wu and Huang in 2009 [60], is the noise-assisted version of EMD, which will be considered as an adaptive mode decomposition method in this research. The essence of both EMD and EEMD is to directly extract intrinsic mode functions (IMFs) with various intrinsic time scales, which is based on local characteristics of target data. Since the intrinsic mode function can reveal the oscillation mode that is embedded in the target data, the EMD and EEMD are employed in this study to identify the intrinsic oscillatory modes in mixed structural response recorded by each sensor. Hence, the data can be decomposed subsequently according to their characteristic timescales for further blind separation.

To understand the theoretical background of EMD and EEMD, the matrix ***S*** in Equation 1 is taken as an example. ***S*** contains all sensor measurements, where the indices n_s and n_t represent the number of sensors and data points in the time domain, respectively. Each column records, $S_i(t)$, can be decomposed into a collection of intrinsic mode functions (IMFs), designated as $\sum_{k=1}^{K} C_k$ in Equation 2, by utilizing EMD/EEMD.

$$S = \begin{bmatrix} S_1(t_1) & \cdots & S_{n_s}(t_1) \\ \vdots & \ddots & \vdots \\ S_1(t_{n_t}) & \cdots & S_{n_s}(t_{n_t}) \end{bmatrix} \quad (1)$$

$$S_i(t) = \sum_{k=1}^{K} C_k, i = 1,2,\Lambda\ , n_s \quad (2)$$

The flowchart of EEMD can be found in Fig. 2.The ensemble sifting time is designated as N_{trial}.The final collection of IMFs, C_{Ntrial}, is the ensemble mean of total trails, shown in Fig. 2(a), while Fig. 2(b) lists the sifting processes of each trail. As a noise-assisted method, the added white noise strength is defined by noise signal ratio, designated as *NSR*, which is the ratio of standard deviation between added noise (σ_{noise}) and target signal (σ_{signal}), given in Equation 3. The recommended *NSR* value is 0.2 [60], which means the assisted noise has the 0.2 times standard deviation as target signal. However, the recommended *NSR* value will be validated in this research. Therefore, the EMD process is without noise, i.e. $NSR = 0$ and with only one trail.

$$NSR = \frac{\sigma_{noise}}{\sigma_{signal}} \quad (3)$$

As mentioned, the purpose of deposing target signal into a group intrinsic mode functions (IMFs) is to provide components whose instantaneous frequencies have physical meaning. Therefore, a satisfactory IMF should meet the necessary conditions when defining a meaningful instantaneous frequency. Hence, two essential conditions should be satisfied by a qualified intrinsic mode function of sensor measurements, as the first judgement process shown in Fig. 2(b). The first condition is the difference of extrema points number and zero crossings number should less than or equal to one in the whole sifted data set, designated as ***h*** in Fig. 2(b). The second rule is the mean value of the upper envelop, e_1, and the lower envelop, e_2, is zero. To stop the sifting process, the residue, r_n should be a monotonic function, which means no more IMF can be extracted from r_n. Readers who are interested in further theoretical background of EMD and EEMD may refer to the papers [59,60].

The results of mode decomposition, no matter employing EMD or EEMD, are a collection of IMFs, C_{final}, which will be dimensionally reduced by PCA before applying blind separation method.

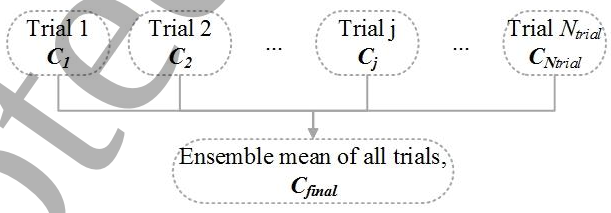

(a) Ensemble empirical mode decomposition theoretical model: final ensemble mean trial

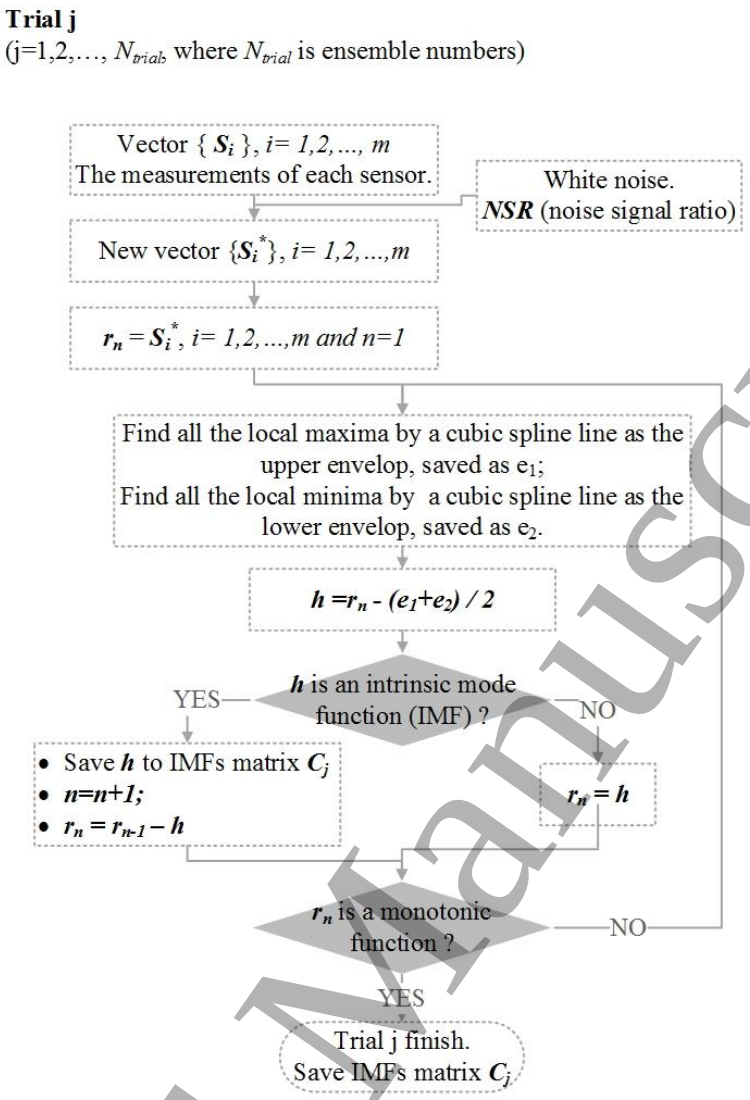

(b) Ensemble empirical mode decomposition theoretical model: single trial

Fig. 2. Ensemble empirical mode decomposition theoretical model

2.2 Data reduction

To compress the size of finial intrinsic mode functions, the matrix C_{final} is interpreted by principal component analysis (PCA). The reformed new variables are called principal components. There are some specific features of those principal components, such as:

- All the principal components are uncorrelated and orthogonal to each other;
- All the principal components are ordered, which means the 1st principal component has the largest possible variance, while the last one has the smallest variance.

The data to be analysed by PCA function is the final collection of intrinsic mode functions, matrix C_{final}, which is the output from mode decomposition. Each column in C_{final} represents an intrinsic mode functions, and overall component number is recorded as n_c. For the sake of simplicity, the set of C_{final} is modified into a vector of IMFs, abbreviated as a vector-matrix notation c.

The principal component analysis is firstly calculating the covariance matrix of c. The variance of this covariance matrix is of interest. Its eigenvectors are subsequently obtained and sorted in the descending order of their corresponding eigenvalues. Thus, the original data set, c, can be reconstructed into a smaller data set, designated as the principal components.

The covariance matrix of the original data c can be termed as matrix V, and the eigenvector of V is abbreviated as matrix D ,whose columns are rearranged according to V 's eigenvalues, from the highest eigenvalue to the lowest. Then, the first m columns of D, which can account for over 95% of the variance, will be saved as the transform matrix A and the original data c will be transformed to the new principal components matrix, P, which contains m orthogonal principal components, often abbreviated as PCs.

Those PCs will then be used for blind separation. The substantial descriptions of PCA can be found in [36].

2.3 Blind separation

Blind separation stresses the following two facts that the source signals (i.e. structural response due to temperature fluctuations or traffic load or wind) are not observed and no prior information is available about the mixed signal. The independent component analysis, or ICA, is the most popular solution for blind separation problem which is used in this paper. The new independent components are obtained by maximizing the nongaussianity, because the nongaussian is independent according to Hyvarinen [61] Hyvarinen explained that a sum of two independent random variables has a closer gaussian distribution compared to any original component. Therefore maximizing the nongaussianity of estimators could get the independent components. The measure of nongaussianity is the extrema of Kurtosis, also known as fourth-order cumulant [61]. Further information about more other measure of non gaussianity can be found in Chapter 8 in Hyvarinen's book. The following part will describe the theoretical background of ICA briefly.

The collection of observations, matrix *S*, in Equation 1 can be given as an example to explain ICA. Equation 4 shows the transposition process of matrix *S*, where the indices *t* is the sample index that equals to $1,2,\dots,n_t$.

$$S^T = \begin{bmatrix} S_1(t_1) & \cdots & S_1(t_{n_t}) \\ \vdots & \ddots & \vdots \\ S_{n_s}(t_1) & \cdots & S_{n_s}(t_{n_t}) \end{bmatrix} = \begin{pmatrix} S_1(t) \\ \vdots \\ S_{n_s}(t) \end{pmatrix} \tag{4}$$

The observations can be assumed as the linear mixture of independent components S^*, abbreviated as ICs, which are shown in Equation 5.

$$\begin{pmatrix} S_1(t) \\ \vdots \\ S_{n_s}(t) \end{pmatrix} = M \begin{pmatrix} S_1^*(t) \\ \vdots \\ S_{n_s}^*(t) \end{pmatrix} \tag{5}$$

Where M is some unknown mixing matrix and n_s^* is the number of latent independent components, which might not be equal to observed mixtures. To simplify ICA estimation, centring and whitening the observable variables are the two necessary pre-processing steps; details can be find in [61]. Since independent component analysis is a mature algorithm, more details can be found in Hyvärinen's work. However, two ambiguities of ICA must be mentioned as it will be used in next numerical model analysis section. The first is that the independent components (ICs) may have different magnitude when compared with observable data. This is because the scalar change can somehow cancel between $s_i^*(t)$ and the corresponding column m_i in mixing matrix M. For example, Equation 5 is simplified by vector-matrix notation, see Equation 6. If $s_i^*(t)$ is multiplied by Δ_i, the effect can be offset by dividing m_i with the same scalar, as showing in Equation 7.

$$S = MS^* = \sum_{i=1}^{n} m_i s_i^* \tag{6}$$

$$S = \sum_{i=1}^{n} m_i s_i^* = \sum_i \left(\frac{1}{\Delta_i} m_i \right) \left(s_i^* \Delta_i \right) \tag{7}$$

Therefore, the variances and magnitude of the ICs cannot be guaranteed and determined. The solution for this restriction is to fix the magnitudes of ICs with unit variance, which means $E(s_i^*, s_i^*) = 1$.

However, an inevitable sign of this ambiguity is the ICs which might be opposite to the corresponding latent variables, i.e. multiplied by -1, which fortunately is insignificant in most applications [61]. Another restriction is the order of independent components that cannot be controlled as the elements in the sum in Equation 6 can be arrayed freely.

2.4 Damage detection

The algorithm MPCA is designed to figure out the characteristics of a certain time series measurements. This certain period record was named as the initialization phase, in which the structure is supposed to be in health condition. After that, anomalous behaviours can be identified according to this initial phase. This certain period is also denominated as window size. The covariance matrix of data inside an active window is calculated and then moving in time, more details can be found in [56,57]

With the moving window, the computational cost is lower for each step and detection of the presence of new situations is timelier because old measurements do not buffer results. The window size should be sufficiently large, so that the periodic variability, i.e. the seasonal temperature cycles, can be exposed, while rapidity of computation can be guaranteed at the same time. Therefore, the window size should be theoretically multiple of periodic variability. In the following numerical simulation, one-year window is chosen in this paper considering lower computational cost, instead of two-year window size in [54], because integrated and continuous measurements can be obtained. After selecting window size, the first principal component, i.e. the eigenvector related to the main eigenvalues, is analysed at each step. The standard deviation of eigenvectors from the first set of data within the fixed window is recorded as σ, which is subsequently used for threshold definition. According to previous researches [54,56], the confidence interval is defined as 3σ off the initial data's eigenvectors.

3 Numerical feature extraction

3.1 Numerical model introduction

The down scaled aluminium bridge for simulation is modelled in ANSYS in previous research [62], whose principal features are shown in Table 1. The monitoring chords are 35 cm long, whose strain will be collected, registered as SG1, SG2, SG3 and SG4 in Fig. 3. The bridge is fixed in all directions at supporting ends A, B, C and D.

Table 1. Principal features of Aluminium Bridge

Young's modulus	Density	Poisson ration	Thermal expansion
$70\ GPa$	$2.7g \cdot cm^{-3}$	0.35	$23.1\ \mu m \cdot m^{-1} \cdot K^{-1}$

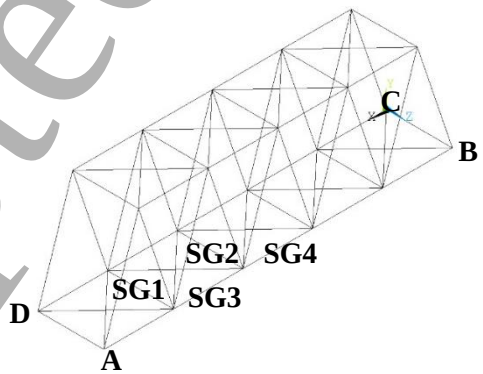

Fig. 3. Truss bridge diagram

The simulated temperature variations are given in Fig. 4(a). The key values are as follows: (1) the average temperature is 9.7℃; (2) maximum daily fluctuation is 4℃ and maximum annual fluctuation is 7℃; (3) the uniform temperature loading is applied on the whole structure; (4) every load step represents 2.5 hours, as three days are selected from each month and 36 days cycles are simulated among 365 load steps.

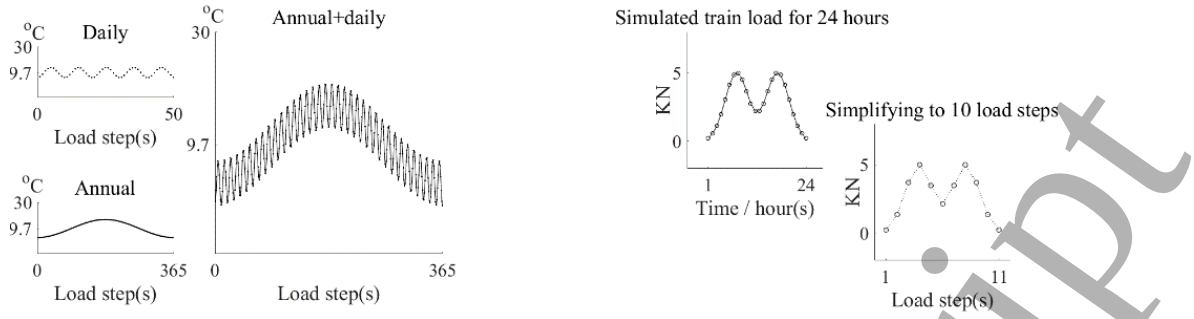

(a) Temperature variations/load (b) Traffic load

Fig. 4. Simulated loading conditions

A time-varying traffic load, with morning and evening peaks, is also simulated and applied at all bottom nodes of the bridge model, showing in Fig. 4(b). The 24-hour traffic load variation conforms to a normal distribution with double peaks, with maximum 5 KN on each bottom node. Since every load step simulates as 2.5 hours, 10 data points are simulated as daily cycle (i.e. 24-hour traffic load variation).

3.2 Thermal feature extraction

The bridge is in healthy condition (i.e. no damage) and exposed to traffic load and thermal load, as shown in Fig. 4. The strain measurements of four monitored beams are permanently recorded, as shown in Fig. 5. The target of the proposed feature extraction method is to extract temperature-induced strain from the mixed structural response. To investigate the feasibility of this method, the discussion will be delivered in two parts: seasonal thermal-effect extraction, and daily thermal-effect extraction, within which the proposed EPI (EMD+PCA+ICA) and EEPI (EEMD+PCA+ICA) will be evaluated and compared. The organization of this sub-section can be found in Fig. 6.

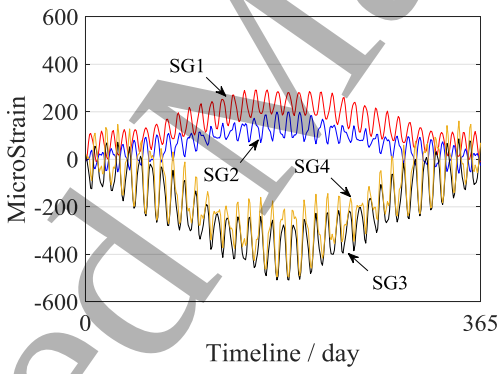

Fig. 5. Mixed structural strain under temperature and traffic loading conditions

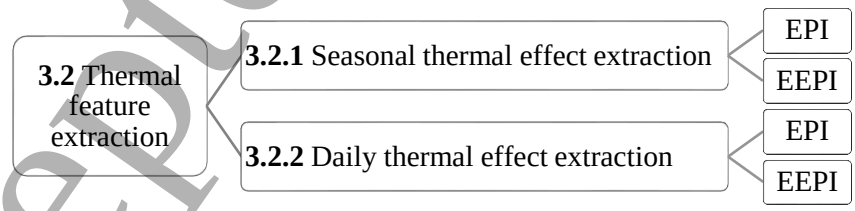

Fig. 6. Organization of Section 3.2

3.2.1 Seasonal thermal-effect extraction

This section will give an assessment and comparison between EPI and EEPI for extracting seasonal temperature-induced strain. The input data, shown in Fig. 5, is normalized for later processing.

EPI, first of all, is applied to one-year (i.e. 365-day duration) mixed structural strain sequence. The extracted seasonal thermal response does not match the ideal strain, as shown in Fig. 7 (a). Ideal seasonal temperature-induced strain is obtained by applying seasonal thermal load only on this bridge.

The correlation coefficient values between them are summarized in Fig. 8 and Table 2, with an alternative assessment value, relative root mean square error (RRMSE). From Fig. 7. (a), it is apparent that one-year data is not enough to extract seasonal thermal effects, as the correlations are all below 0.63 and RRMSE is quite high, over 78%.

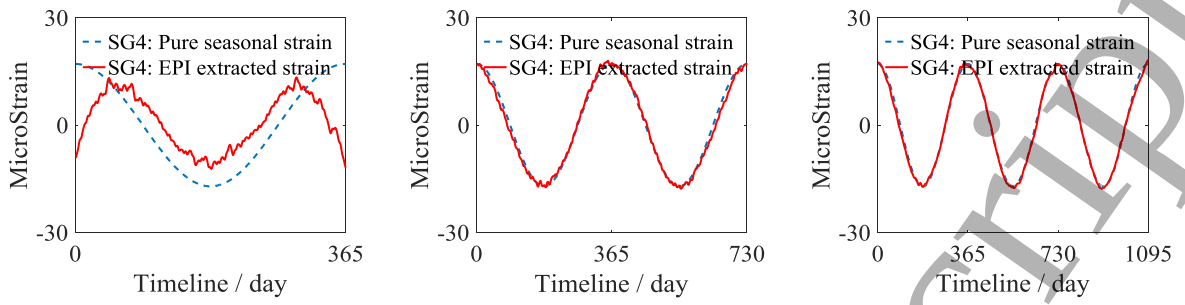

(a) SG4: one-year duration (b) SG4: two-year duration (c) SG4: three-year duration

Fig. 7. Seasonal thermal-strain separated by EPI: one-year/two-year/three-year measurements

Considering that the seasonal pattern of temperature variations can only become visible when the time duration is over two years or even longer, then two-year and three-year mixed structural measurements are analysed by EPI. The time-history comparison between estimated and ideal temperature-induced strains is given in Fig. 7 (b) and Fig. 7 (c), whose coefficient correlation and root mean square error are summarized in Fig. 8 and Table 2. For two-year duration simulation, the correlation ranges from 0.94 to 0.99 for all target beams, which shows a higher improvement than previous separation. If enlarging the sample size to three years, a visible amendment for SG2 can be observed with the higher correlation and lower RRMSE values, referring to Fig. 8.

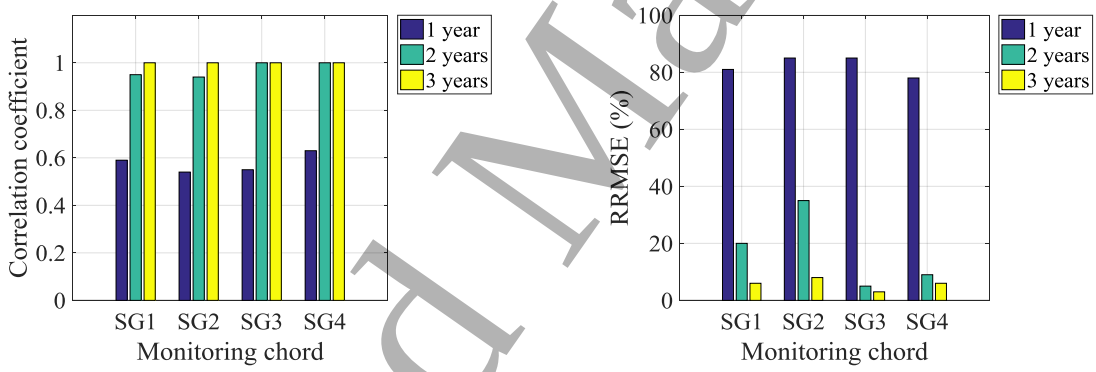

(a) Correlation coefficient (b) Relative Root Mean Square Error

Fig. 8. Summary of seasonal thermal strain extraction by EPI

Table 2. Summary of seasonal thermal-effect separated by EPI

	Correlation coefficient				Relative root mean square error			
	SG1	SG2	SG3	SG4	SG1	SG2	SG3	SG4
One-year data	0.59	0.54	0.55	0.63	81%	85%	85%	78%
Two-year data	0.98	0.94	1.00	1.00	20%	35%	5%	9%
Three-year data	1.00	1.00	1.00	1.00	6%	8%	3%	6%

Results demonstrate that the extracting capacity of EPI is related to the target signal's length. With one-year data, as the 365 bar showing in Fig. 8, the separating results are not satisfactory. The correlations are all below 0.63, as 0.59, 0.54, 0.55 and 0.63 for SG1-4 respectively, while the relative root mean square errors are quilt high, around 80%. However, the separation results have a significant improvement when applying EPI to two-year strain measurements. In addition, the extracting results will be slightly enhanced when the cycles are enlarged from two years to three years. The correlation values are all reaching up to 1.00 for all the monitored beams and the relative root mean square error decreases to 3%. The other advantage is the computational cost does not have any change while changing the size of the target signal. Therefore, EPI is qualified enough for separating seasonal

temperature response from at least two years measurements. The following part of this section will give the simulation results by applying EEPI and comparing it with EPI.

Considering the previous results, the EPI is trustworthy and efficient enough when the target sources are over two-year duration, so the EEPI will not be recommended for these cases, because of the higher computation cost when compared with EPI. Only one-year mixed strain is utilized for performing EEPI to extract seasonal temperature-induced strain, since the EPI fails in this case. When applying EEPI, the ensemble empirical mode decomposition (EEMD) is selected to decompose target single-channel signal. As a result, two parameters, *NSR* (noise-signal ratio) and *N* (the number of trails) have a significant influence on the final separation results. Therefore, a series of *NSR* and *N* combinations are selected for their impact research, at a very high computational cost when compared with EPI.

The extracting results that are obtained by using various *NSR* and *N* values in EEMD have been compared with ideal temperature-induced structural strain for each monitored beam. The assessments about *NSR* and *N* are delivered in Fig. 9.

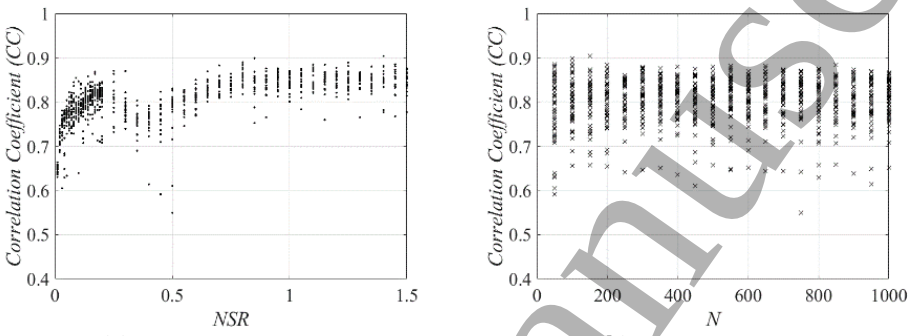

(a) SG4: *NSR* impact (b) SG4: *N* impact

Fig. 9. EEPI: the impact of *NSR* (noise-signal ratio) and *N* (the number of trails) for extracting SEASONAL thermal-strain.

From Fig. 9, it is evident that *NSR* has an obvious effect on the performance of EEPI (EEMD+PCA+ICA), while *N*'s impact is less significant. Among all the evaluation results, the best combination of *NSR*=1.1 and *N*=850 is found out to achieve the optimal separation performance.

Fig. 10 shows the comparison between estimated strain, separated by EEPI, and ideal strain, induced by applying annual temperature load only. The seasonal thermal strain is not recovered very well. The correlation coefficient values are 0.85, 0.85, 0.86 and 0.84, while RRMSE are 56%, 57%, 54% and 58% for SG1-4 respectively, which is not high enough but much better than EPI's performance on one-year monitoring data. As aforementioned, EPI is efficient enough to extract seasonal temperature effects when the measurements are recorded over two years. Therefore, EEPI can be treated as an alternative method when the measurement sources are limited.

Comparing the separated results by EPI and EEPI, the following three highlights can be summarized for the seasonal case.

- EPI can recover seasonal temperature-induced strain at a compelling level, with 0.99 correlation and lower computational cost. However, it fails when the target strain is only one-year measurements;
- EEPI performs better than EPI when monitoring data is less than two years; Because the EEPI separation results show higher correlation coefficient and lower relative root mean square error when compared with EPI extracting performance;
- Due to the large computational calculation of EEPI, it is not recommended for the case when target signal is over two-year records.

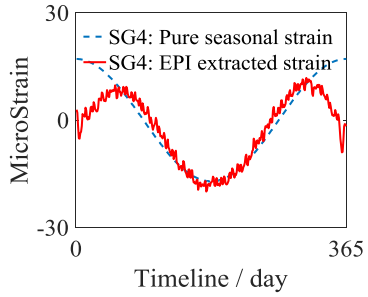

Fig. 10. Seasonal thermal-strain separated by EEPI (*NSR=1.1, N=850*)

Table 3. Comparisons of seasonal thermal-strain extraction by EPI and EEPI

Time duration	**365**							
Method	**EPI**				**EEPI**			
Strain Gauge No.	SG1	SG2	SG3	SG4	SG1	SG2	SG3	SG4
Correlation coefficient	0.59	0.54	0.55	0.63	0.85	0.85	0.86	0.84
Relative Root Mean Square Error	81%	85%	85%	78%	56%	57%	54%	58%

3.2.2 Daily thermal-effect extraction

Similar to the seasonal case, the assessment will be discussed as the following three parts: a) EPI for recovering daily temperature effects; b) EEPI for predicting daily temperature strain; c) comparison between EPI and EEPI.

In the previous section, the performance of EPI method is influenced by the data size, i.e. to separate seasonal thermal effect, the measurement duration should be no less than the longest variation period. Hence, only one year data is adequate for daily case, since 36 daily cycles are simulated within one year, which can be confirmed from Fig. 11. According to Fig. 11, the correlation values for SG1-4 are 0.97, 0.84, 0.94 and 0.81 correspondingly, while the corresponding relative root mean square errors are 36%, 54%, 35%, 59%. The separating results from SG1 and SG3 are slightly better than SG2 and SG4. It is also apparent that various data length has slightly influence on the final results.

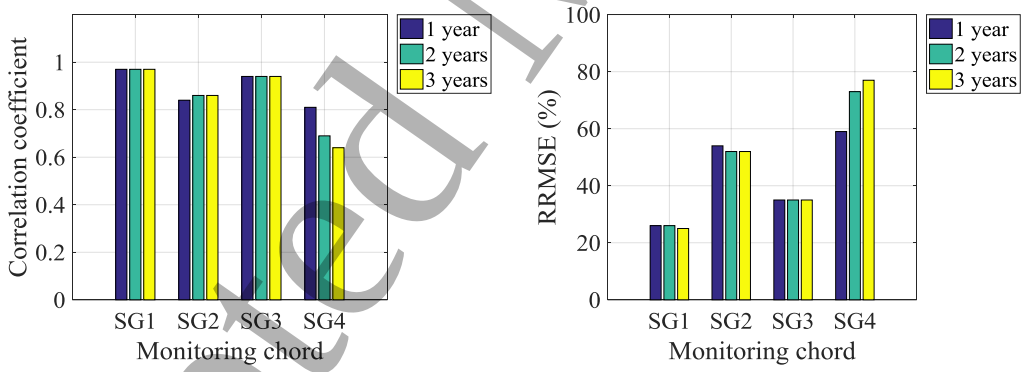

Fig. 11. Evaluation of EPI for DAILY thermal strain extraction

Fig. 12 (a) shows these extracted signals for each monitored chord in the time domain. To have a clear view of the separated results, Fig. 12 (b) shows the separating results in another view, the relation between temperature and strain.

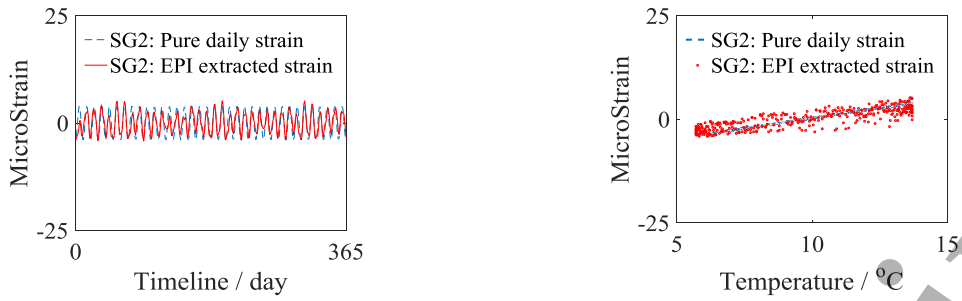

(a) SG2: strain measurements in time domain (b) SG2: strain-temperature relation

Fig. 12. Daily thermal-strain separated by EPI (one-year measurements)

For evaluating the performance of EEPI for daily thermal issues, the research of how *NSR* (noise-signal ratio) and *N* (the number of trails) affect the final blind separation results will be given first. Similar as the previous part of seasonal strain recovery, Fig. 13 gives an overview of the relationship among *NSR*, *N* and separating results. The SG2 is taken as an example.

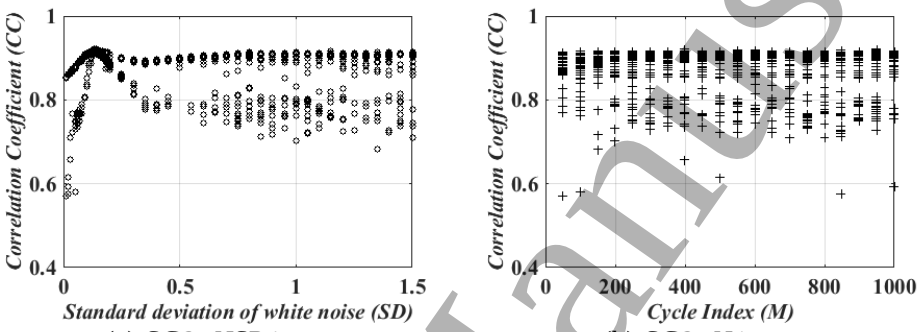

(a) SG2: *NSR* impact (b) SG2: *N* impact

Fig. 13. EEPI: the impact of *NSR* (noise-signal ratio) and *N* (the number of trails) for extracting DAILY thermal-strain

Referring to Fig. 13, *NSR* has an obvious effect on the performance of EEPI (EEMD+PCA+ICA), while *N* has a slight influence on the final separating results. When *NSR* is around 0.2, the blind separation results are reaching the peak value and stable for all monitored beams. The correlation coefficient results are generally around 0.80, according to Fig. 13. And the recommended combination of *NSR=0.11* and *N=400*. Fig. 14 (a) shows the extraction results in the time domain and their comparison with ideal strain, while Fig. 14 (b) shows the relation between temperature and temperature-induced strain.

According to above evaluation on EPI and EEPI for extracting daily temperature-induced variations, EEPI has an evident improvement and relative higher robustness for extracting daily thermal strain based on following two points.

- As displayed in Table 4, the performance of EPI shows 0.81-0.97 correlation value, while EEPI increases them to 0.91-0.96.
- Regarding the relative root mean square error, EEPI not only decreases EPI's result value (35%-59%) to 28%-42%, but also narrows the range, which means EEPI is more robust than EPI.

The capability of EEPI method to separate thermal strain will be also evaluated in the next section.

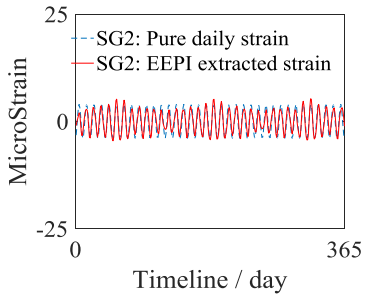

(a) SG2: strain measurements in time domain

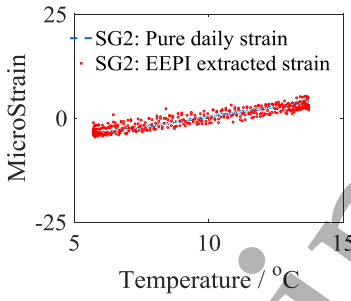

(b) SG2: strain-temperature relation

Fig. 14. Daily thermal-strain separated by EEPI (one-year measurements)

Table 4. EEPI: evaluation of daily thermal-strain extraction (*NSR=0.11*, *N=400*)

Time duration	**365**							
Method	**EPI**				**EEPI**			
Strain Gauge No.	SG`1	SG2	SG3	SG4	SG1	SG2	SG3	SG4
Correlation coefficient	0.97	0.84	0.94	0.81	0.98	0.91	0.96	0.91
Relative Root Mean Square Error	26%	54%	35%	59%	18%	41%	28%	42%

4 Truss bridge case study

The aluminium truss bridge model was built in Structural Laboratory in School of Engineering of University of Warwick. The bridge test setup is shown in Fig. 15. There are four heating lamps on the top of this truss structure. The four ends are fixed with one steel bar going through the gusset plates of the bridge and fixed on the Meccano.

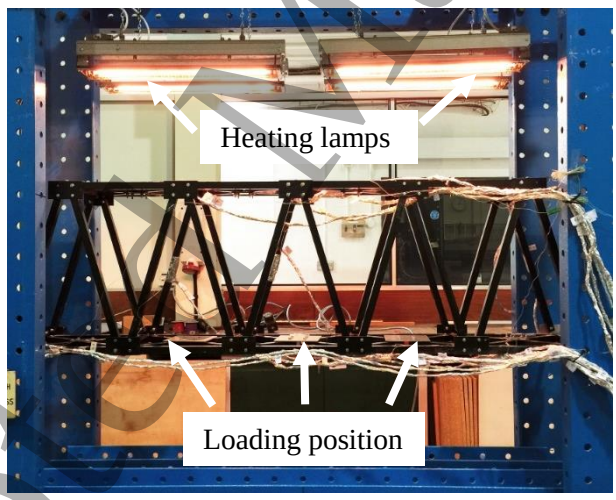

Fig. 15. The truss bridge model in Structural Laboratory in University of Warwick

The truss dimension and the sensors of interest in this paper can be found in Fig. 16. Four strain gauges from bottom chords, designated as SG-1 to SG-4, are selected for this case study because they are close to loading position, where weight loading condtion has a more comparable effect. There have three thermcouples attached close to four strain gauges, notated as TH-A to TH-C. The SG1 is attached on the top surface of the longitudinal chord, while SG2 is attached on the bottom surface of the transversal chord. Both SG-3 and SG-4 are attached on the bottom surface of the target chords to avoid the direct radiation of heating lamps.

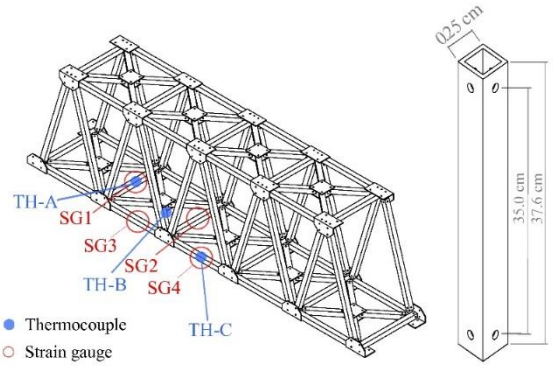

Fig. 16. Monitoring system and monitored chord dimension

4.1 Thermal feature separation

To evaluate the performance of the EEPI and EPI methods for thermal feature separation, two groups of test, reference test and hybrid test, are taken when the bridge is in health condition.

- Reference test: only temperature load is applied on the bridge. The temperature variations are between 16 to 20 ℃, seeing Fig. 17 (a). The linear relation between temperature and strain can be obtained, which is the basis rule to evaluate the performance of the proposed EEPI or EPI, as showing in Fig. 17 (b).
- Hybrid test: the combined time-varying temperature and weight load are applied on the bridge. The temperature keeps fluctuating within 16-20 ℃, seeing Fig. 18. The 30 Kg weights are distributed into three loading positions, as shown in Fig. 15. The strain is labelled as mixed strain, using ε_{all}, which is then analyzed by EEPI and EPI to obtain the estimated strain, termed as ε_{es}.

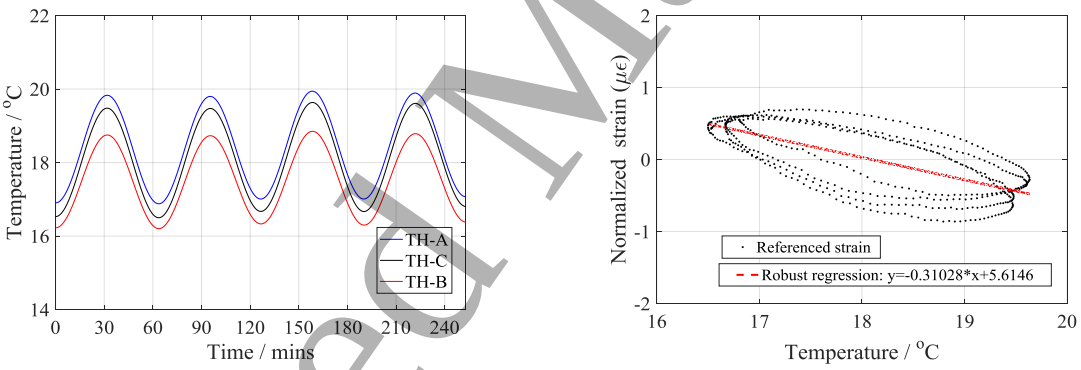

(a). The temperature records in reference test

(b). The strain-temperature relation in reference test (SG4 vs. TH-C)

Fig. 17. Temperature and strain measurements in reference test

For brevity, only SG4 will be presented here for feature extraction. The EPI is evaluated first, whose separated results in the time domain are presented in Fig. 19(a), while EEPI extracted results are given in Fig. 19(b). Apparently, the EEPI can reveal the 2.5 circulations in the time domain, while the EPI could not. Since the reference test has confirmed the linear relation between temperature and strain, the correlation of the ε_{es} with relative temperature records is selected to assess the method's performance. The correlation with temperature variations are 0.64 and 0.71 by EPI and EEPI respectively. In other words, the higher correlation coefficient with temperature fluctuation, the better separation. Therefore, the EEPI could separate thermal feature more properly than EPI.

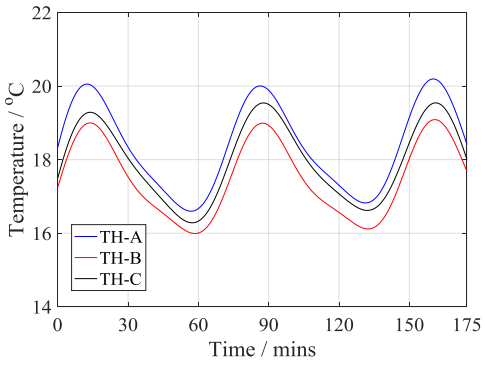

Fig. 18. Temperature variations in hybrid test.

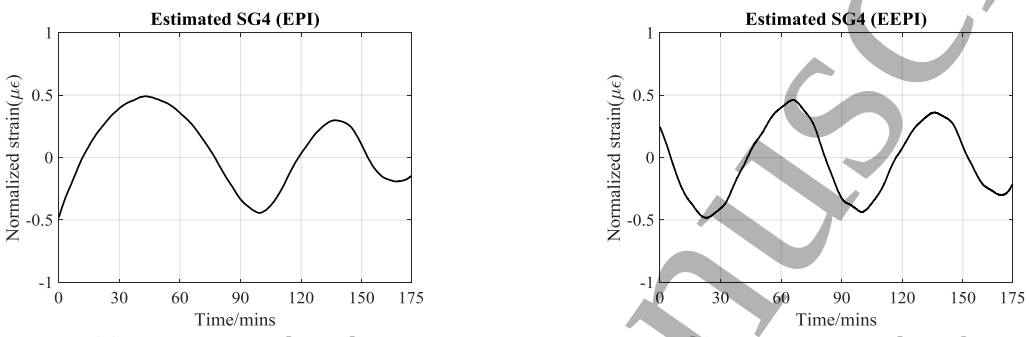

(a) EPI estimated result (b) EEPI estimated result

Fig. 19. The estimated strain for SG4 by EPI and EEPI (*NSR=0.11* and *N=400*)

4.2 Damage detection

The damage is introduced in the bottom chord of the middle span, which is opposite to SG4, as shown in Fig. 20. The first level of damage is removing the target chord followed by the second level is loosening the transversal connection next to the absent chord. The similar hybrid test will be conducted on the bridge, i.e. temperature and weight loadings. The MPCA will be applied on the separated thermal response for the purpose of damage detection.

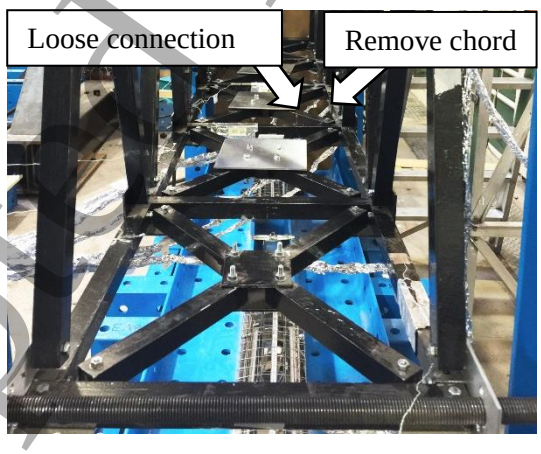

Fig. 20. The damage condition in truss bridge.

The time points of interest are as follows and will be shown in following figure.

- L1: the starting time of removing target chord;
- L2: the target chord is totally removed;
- L3: loosening connection next to the absent chord.

The strain measurements from SG4 is given as an example in Fig. 21. For the mixed structural response, it is difficult to identify the damage. The detection results by applying MPCA directly are also invisible as shown in Fig. 22 (a). However, the proposed EEPI can make an improvement. Fig. 22 (b) shows the MPCA results on the extracted thermal strain, which is separated by EEPI. The sharp changes can be observed during L1 and L2, which stands for the influence when moving chord. And the peaks after L2 obviously indicate that the damage has been detected.

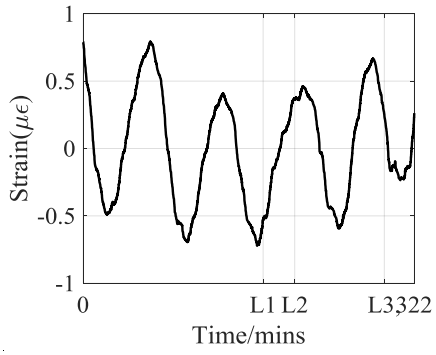

Fig. 21. The original SG4 measurements in time domain (with damage).

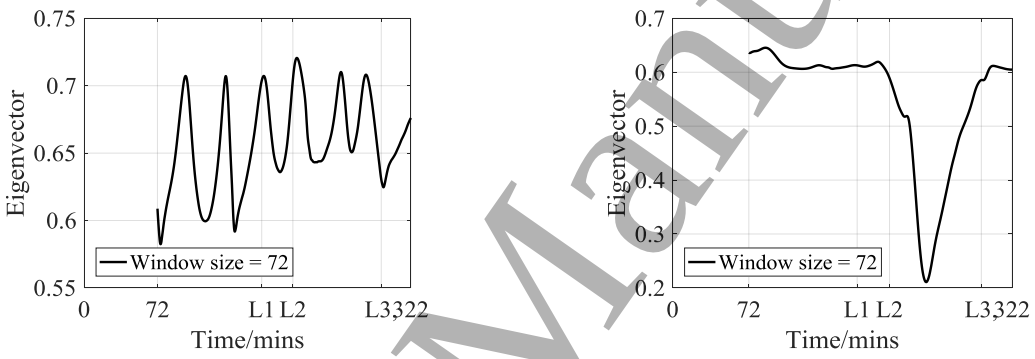

(a) MPCA on original strain measurements (b) MPCA on EEPI separated strain

Fig. 22. Damage detection outcomes.

5 Concluding remarks

In this study, a combined data interpretation method based on single-channel blind signal separation has been proposed for thermal feature extraction, followed by an investigation to evaluate its potential ability to detect structural damage.

Due to the different choice for mode decomposition, this research compares the performance of EMD+PCA+ICA, termed as EPI, and EEMD+PCA+ICA, termed as EEPI. Both are employed for extracting seasonal and daily thermal strain sequences. According to the assessment results, some conclusions can be summarized as follows.

- EPI is robust enough with higher capacity for separating seasonal temperature effects, only if monitoring measurements are over two years. Otherwise, EEPI will be an alternative and trustworthy option for extracting seasonal thermal strain;
- To extract daily thermal impact, EEPI has shown higher robustness and accuracy, when compared with EPI;
- The extracted temperature effects show a potential ability to detect damage by applying MPCA. However, further research with various damage levels is required.

Acknowledgement

This work was supported by the British Council (Grant ID: 217544274) and China Scholarship Council.

References

[1] Farrar C R and Worden K 2007 An introduction to structural health monitoring *Philos. Trans. R. Soc. A Math. Phys. Eng. Sci.* **365** 303–15

[2] Sohn H, Farrar C R, Hemez F M, Shunk D D, Stinemates D W, Nadler B R and Czarnecki J J 2003 *A review of structural health monitoring literature: 1996--2001*

[3] Brownjohn J M W 2007 Structural health monitoring of civil infrastructure *Philos. Trans. R. Soc. A Math. Phys. Eng. Sci.* **365** 589–622

[4] Valinejadshoubi M, Bagchi A and Moselhi O 2016 Structural Health Monitoring of Buildings and Infrastructure *Int. J. Civ. Eng. Technol.* **10** 731–8

[5] Gomes G F, Mendéz Y A D, da Silva Lopes Alexandrino P, da Cunha S S and Ancelotti A C 2018 The use of intelligent computational tools for damage detection and identification with an emphasis on composites – A review *Compos. Struct.* **196** 44–54

[6] Li H-N, Ren L, Jia Z-G, Yi T-H and Li D-S 2016 State-of-the-art in structural health monitoring of large and complex civil infrastructures *J. Civ. Struct. Heal. Monit.* **6** 3–16

[7] Ko J M and Ni Y Q 2005 Technology developments in structural health monitoring of large-scale bridges *Eng. Struct.* **27** 1715–25

[8] Wong K-Y 2007 Design of a structural health monitoring system for long-span bridges *Struct. Infrastruct. Eng.* **3** 169–85

[9] Koo K Y, Brownjohn J M W, List D I and Cole R 2013 Structural health monitoring of the Tamar suspension bridge *Struct. Control Heal. Monit.* **20** 609–25

[10] Yarnold M T, Moon F L and Emin Aktan A 2015 Temperature-Based Structural Identification of Long-Span Bridges *J. Struct. Eng.* **141** 4015027

[11] Sohn H 2007 Effects of environmental and operational variability on structural health monitoring *Philos. Trans. R. Soc. A Math. Phys. Eng. Sci.* **365** 539–60

[12] Wood M G 1992 *Damage analysis of bridge structures using vibrational techniques* (University of Aston in Birmingham)

[13] Moorty S and Roeder C W 1992 Temperature-Dependent Bridge Movements *J. Struct. Eng.* **118** 1090–105

[14] Peeters B and De Roeck G 2001 One-year monitoring of the Z24-Bridge: environmental effects versus damage events *Earthq. Eng. Struct. Dyn.* **30** 149–71

[15] Nguyen V H, Schommer S, Maas S and Zürbes A 2016 Static load testing with temperature compensation for structural health monitoring of bridges *Eng. Struct.* **127** 700–18

[16] Helmicki A, Hunt V, Shell M, Lenett M, Turer A, Dalal V and Aktan A 1999 Multidimensional performance monitoring of a recently constructed steel-stringer bridge *2nd international workshop on structural health monitoring* (Stanford University, Palo Alto, CA) pp 408–16

[17] Catbas F N, Susoy M and Frangopol D M 2008 Structural health monitoring and reliability estimation: Long span truss bridge application with environmental monitoring data *Eng. Struct.* **30** 2347–59

[18] Cross E J, Koo K Y, Brownjohn J M W and Worden K 2013 Long-term monitoring and data analysis of the Tamar Bridge *Mech. Syst. Signal Process.* **35** 16–34

[19] Ding Y and Li A 2011 Temperature-induced variations of measured modal frequencies of steel box girder for a long-span suspension bridge *Int. J. Steel Struct.* **11** 145–55

[20] Jin C, Li J, Jang S, Sun X and Christenson R 2015 Structural damage detection for in-service highway bridge under operational and environmental variability *SPIE Smart Structures and Materials+ Nondestructive Evaluation and Health Monitoring* ed J P Lynch p 94353A

[21] Kromanis R and Kripakaran P 2014 Predicting thermal response of bridges using regression models derived from measurement histories *Comput. Struct.* **136** 64–77

[22] Kromanis R and Kripakaran P 2016 SHM of bridges: characterising thermal response and detecting anomaly events using a temperature-based measurement interpretation approach *J. Civ. Struct. Heal. Monit.* **6** 237–54

[23] Yarnold M, Murphy B, Glisic B and Reilly J 2016 Temperature-Based Evaluation and Monitoring Techniques for Long-Span Steel Bridges *Transportation Research Board 95th Annual Meeting*

[24] Zhou L, Xia Y, Brownjohn J M W and Koo K Y 2016 Temperature Analysis of a Long-Span Suspension Bridge Based on Field Monitoring and Numerical Simulation *J. Bridg. Eng.* **21** 4015027

[25] Sohn H, Worden K and Farrar C R 2002 Statistical Damage Classification Under Changing Environmental and Operational Conditions *J. Intell. Mater. Syst. Struct.* **13** 561–74

[26] Yan A-M, Kerschen G, De Boe P and Golinval J-C 2005 Structural damage diagnosis under varying environmental conditions—part II: local PCA for non-linear cases *Mech. Syst. Signal Process.* **19** 865–80

[27] Bellino A, Fasana A, Garibaldi L and Marchesiello S 2010 PCA-based detection of damage in time-varying systems *Mech. Syst. Signal Process.* **24** 2250–60

[28] Wah W S L, Chen Y-T, Roberts G W and Elamin A 2017 Damage Detection of Structures Subject to Nonlinear Effects of Changing Environmental Conditions *Procedia Eng.* **188** 248–55

[29] Miao Q, Wang D and Pecht M 2011 Rolling element bearing fault feature extraction using EMD-based independent component analysis *2011 IEEE Conference on Prognostics and Health Management* (IEEE) pp 1–6

[30] Žvokelj M, Zupan S and Prebil I 2016 EEMD-based multiscale ICA method for slewing bearing fault detection and diagnosis *J. Sound Vib.* **370** 394–423

[31] Yang J N, Lei Y, Lin S and Huang N 2004 Hilbert-Huang Based Approach for Structural Damage Detection *J. Eng. Mech.* **130** 85–95

[32] OBrien E J, Malekjafarian A and González A 2017 Application of empirical mode decomposition to drive-by bridge damage detection *Eur. J. Mech. - A/Solids* **61** 151–63

[33] Yang Y-B, Lin C W and Yau J D 2004 Extracting bridge frequencies from the dynamic response of a passing vehicle *J. Sound Vib.* **272** 471–93

[34] He W-Y and Zhu S 2016 Moving load-induced response of damaged beam and its application in damage localization *J. Vib. Control* **22** 3601–17

[35] Amezquita-Sanchez J P and Adeli H 2016 Signal Processing Techniques for Vibration-Based Health Monitoring of Smart Structures *Arch. Comput. Methods Eng.* **23** 1–15

[36] Jolliffe I 2011 Principal Component Analysis *International Encyclopedia of Statistical Science* (Berlin, Heidelberg: Springer Berlin Heidelberg) pp 1094–6

[37] Hotelling H 1933 Analysis of a complex of statistical variables into principal components. *J. Educ. Psychol.* **24** 417–41

[38] Huang H, Yi T and Li H 2016 Canonical correlation analysis based fault diagnosis method for structural monitoring sensor networks *Smart Struct. Syst.* **17** 1031–53

[39] Huang H-B, Yi T-H and Li H-N 2017 Bayesian Combination of Weighted Principal-Component Analysis for Diagnosing Sensor Faults in Structural Monitoring Systems *J. Eng. Mech.* **143** 4017088

[40] Loh C-H, Huang Y-T, Hsueh W, Chen J-D and Lin P-Y 2017 Visualization and Dimension Reduction of High Dimension Data for Structural Damage Detection *Procedia Eng.* **188** 17–24

[41] Datteo A, Lucà F and Busca G 2017 Statistical pattern recognition approach for long-time monitoring of the G.Meazza stadium by means of AR models and PCA *Eng. Struct.* **153** 317–33

[42] Sadhu A, Narasimhan S and Antoni J 2017 A review of output-only structural mode

identification literature employing blind source separation methods *Mech. Syst. Signal Process.* **94** 415–31

[43] Nagarajaiah S and Yang Y 2015 Blind modal identification of output-only non-proportionally-damped structures by time-frequency complex independent component analysis *Smart Struct. Syst.* **15** 81–97

[44] Yang Y, Dorn C, Mancini T, Talken Z, Nagarajaiah S, Kenyon G, Farrar C and Mascareñas D 2017 Blind identification of full-field vibration modes of output-only structures from uniformly-sampled, possibly temporally-aliased (sub-Nyquist), video measurements *J. Sound Vib.* **390** 232–56

[45] Comon P 1994 Independent component analysis, A new concept? *Signal Processing* **36** 287–314

[46] Zang C, Friswell M I and Imregun M 2004 Structural Damage Detection using Independent Component Analysis *Struct. Heal. Monit. An Int. J.* **3** 69–83

[47] Poncelet F, Kerschen G, Golinval J-C and Verhelst D 2007 Output-only modal analysis using blind source separation techniques *Mech. Syst. Signal Process.* **21** 2335–58

[48] Yang Y and Nagarajaiah S 2013 Time-Frequency Blind Source Separation Using Independent Component Analysis for Output-Only Modal Identification of Highly Damped Structures *J. Struct. Eng.* **139** 1780–93

[49] Chang J, Liu W, Hu H and Nagarajaiah S 2016 Improved independent component analysis based modal identification of higher damping structures *Measurement* **88** 402–16

[50] Kano M, Tanaka S, Hasebe S, Hashimoto I and Ohno H 2003 Monitoring independent components for fault detection *AIChE J.* **49** 969–76

[51] Wang J, Zhang Y, Cao H and Zhu W 2012 Dimension reduction method of independent component analysis for process monitoring based on minimum mean square error *J. Process Control* **22** 477–87

[52] Li G and Qin S J 2018 Comparative study on monitoring schemes for non-Gaussian distributed processes *J. Process Control* **67** 69–82

[53] Han L, Li C W, Guo S L and Su X W 2015 Feature extraction method of bearing AE signal based on improved FAST-ICA and wavelet packet energy *Mech. Syst. Signal Process.* **62–63** 91–9

[54] Posenato D, Lanata F, Inaudi D and Smith I F C 2008 Model-free data interpretation for continuous monitoring of complex structures *Adv. Eng. Informatics* **22** 135–44

[55] Hubert M, Rousseeuw P J and Vanden Branden K 2005 ROBPCA: A New Approach to Robust Principal Component Analysis *Technometrics* **47** 64–79

[56] Posenato D, Kripakaran P, Inaudi D and Smith I F C 2010 Methodologies for model-free data interpretation of civil engineering structures *Comput. Struct.* **88** 467–82

[57] Laory I, Trinh T N and Smith I F C 2011 Evaluating two model-free data interpretation methods for measurements that are influenced by temperature *Adv. Eng. Informatics* **25** 495–506

[58] Laory I, Trinh T N, Posenato D and Smith I F C 2013 Combined Model-Free Data-Interpretation Methodologies for Damage Detection during Continuous Monitoring of Structures *J. Comput. Civ. Eng.* **27** 657–66

[59] Huang N E, Shen Z, Long S R, Wu M C, Shih H H, Zheng Q, Yen N-C, Tung C C and Liu H H 1998 The empirical mode decomposition and the Hilbert spectrum for nonlinear and non-stationary time series analysis *Proc. R. Soc. A Math. Phys. Eng. Sci.* **454** 903–95

[60] WU Z and HUANG N E 2009 ENSEMBLE EMPIRICAL MODE DECOMPOSITION: A NOISE-ASSISTED DATA ANALYSIS METHOD *Adv. Adapt. Data Anal.* **1** 1–41

[61] Hyvärinen A, Karhunen J and Oja E 2004 *Independent component analysis* (John Wiley & Sons)

[62] Zhu Y, Jesus A H and Laory I 2016 Predicting thermal response for structural health monitoring

using blind source separation method *8th European Workshop On Structural Health Monitoring* pp 2841–52